INTERNATIONAL JOURNAL FOR NUMERICAL METHODS IN FLUIDS
Int. J. Numer. Meth. Fluids 2010; **63**:622–637
Published online 2 July 2009 in Wiley InterScience (www.interscience.wiley.com). DOI: 10.1002/fld.2098

Numerical solution of the two-phase expansion of a metastable flashing liquid jet using the dispersion-controlled dissipative scheme

J. A. J. Avila[1,*,†], M. M. Pimenta[2] and J. R. Simões-Moreira[2]

[1]*Department of Mathematics, Universidade Federal de São João del-Rei, Praça Frei Orlando 170, São João del-Rei, MG 36307-352, Brazil*
[2]*SISEA—Alternative Energy Systems Laboratory, Mechanical Engineering Department, Escola Politécnica, Universidade de São Paulo, São Paulo, SP 05508-900, Brazil*

SUMMARY

This paper presents a study of the stationary phenomenon of superheated or metastable liquid jets, flashing into a two-dimensional axisymmetric domain, while in the two-phase region. In general, the phenomenon starts off when a high-pressure, high-temperature liquid jet emerges from a small nozzle or orifice expanding into a low-pressure chamber, below its saturation pressure taken at the injection temperature. As the process evolves, crossing the saturation curve, one observes that the fluid remains in the liquid phase reaching a superheated condition. Then, the liquid undergoes an abrupt phase change by means of an oblique evaporation wave. Across this phase change the superheated liquid becomes a two-phase high-speed mixture in various directions, expanding to supersonic velocities. In order to reach the downstream pressure, the supersonic fluid continues to expand, crossing a complex bow shock wave. The balance equations that govern the phenomenon are mass conservation, momentum conservation, and energy conservation, plus an equation-of-state for the substance. A false-transient model is implemented using the shock capturing scheme: dispersion-controlled dissipative (DCD), which was used to calculate the flow conditions as the steady-state condition is reached. Numerical results with computational code *DCD-2D v1* have been analyzed. Copyright © 2009 John Wiley & Sons, Ltd.

Received 19 January 2009; Revised 14 April 2009; Accepted 5 May 2009

KEY WORDS: flashing; evaporation waves; two-phase flow; shock wave; conservation equations; dispersion-controlled dissipative scheme; shock capturing schemes

*Correspondence to: J. A. J. Avila, Department of Mathematics, Universidade Federal de São João del-Rei, Praça Frei Orlando 170, São João del-Rei, MG 36307-352, Brazil.
†E-mail: avila_jaj@hotmail.com, avila_jaj@ufsj.edu.br

1. INTRODUCTION

The flashing phenomenon of metastable liquid jets is important for industrial and technological applications. Many theoretical, experimental and computational researches have been developed in order to better understand and predict the fluid behavior undergoing a sudden phase change from liquid to vapor. In this field, mathematical models and predictive computational codes are of particular interest. These models should incorporate sufficient understanding of these phenomena; on the other hand, numerical simulations must be adequate in solving engineering application problems. Some applications of the present study address situations reported in industrial accidents [1], in fuel injection [2], and in safety and relief [3], to mention a few.

Evaporative phenomena have been studied by Simões-Moreira [4] in which he experimentally studied the formation of adiabatic evaporation waves in superheated dodecane ($C_{12}H_{26}$) at laboratory conditions. As this fluid can be classified as a 'retrograde' substance, it may undergo a complete phase change under certain state conditions.

In the theoretical and experimental study of shock formation in superheated liquid jets, one cites: Kurschat *et al.* [5], which studied the evaporation of superheated jets from an expansion nozzle into a vacuum chamber using a fluid of high molecular complexity ('retrograde'), named perfluor-n-hexane (C_6F_{14}), in their tests. Vieira [6, 7] and Vieira and Simões-Moreira [8] built an experimental apparatus to study the behavior of flashing liquid jets into low-pressure environment. The two-phase high-speed expansion region comes to an end due to the formation of an ellipsoid or spheroid shock structure enveloping the liquid jet core. As an example, a shock wave structure occurs during the expansion of a liquid kerosene jet with injection pressure of 600E+03 Pa discharging in a low-pressure chamber at 1.6E+03 Pa. A Schilieren image of this expansion and shock is shown in Figure 1.

In numerical studies of shock wave formation in superheated liquid jets expansion, one may cite: Simões-Moreira *et al.* [9] who analyzes the problem of the shock wave formation in flashing liquid jets from a one-dimensional point-of-view. They employ a one-dimensional hemispherical approach and implement a simple computer code named *ShoWPhasT-1D*—'*shock waves with phase transition*'. With reference to steady flashing of metastable liquid jets in two-dimensional axisymmetric domain, the two-phase region, one has: Angelo [10] who developed the code *ShoWPhasT-2D*. Angelo [11] improved the code, but his new code could not capture directly the shock wave

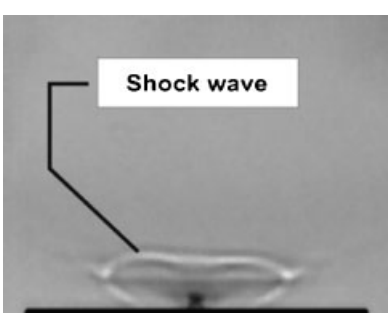

Figure 1. Shock wave formation in kerosene flashing jets, Vieira [6].

DOI: 10.1002/fld

structure and as a result he implemented a capturing scheme algorithm to find the shock location (see also Angelo and Simões-Moreira [12]). An important contribution was the first version of the code: *ShoWPhasT-2D v1*. Avila *et al.* [13] implemented a computational code, named *ShoWPhasT-2D v2*, which is an improved version of previous codes. It has significantly reduced the computational time and obtained a more precise shock wave shape, when compared with the experimental results of Vieira [7]. Avila *et al.* [14] presented similar results. All previous codes were not capable of directly capture the shock wave structure, or additional algorithms are used in the post-processing. Avila [15] implemented the computational code *dispersion-controlled dissipative-two-dimensional version 1* (*DCD-2D v1*), based on the scheme by Jiang [16], which directly captures the shock wave and solves, in general, non-stationary phenomena. In particular, here it resolves the phenomenon, in a two-dimensional axisymmetric domain, correspondent to the two-phase region, assuming a false-transient approach.

2. FLASHING PHENOMENON

Flashing of superheated evaporative jets is a stationary three-dimensional phenomenon, in which the liquid at the stagnation condition undergoes six relevant thermodynamic states, which can be divided in a *pre-two-phase* region and a *two-phase* region. The states in the *pre-two-phase* region are: initial state (reservoir state), denoted by (0); superheated state (or metastable), denoted by (1); and post-evaporation wave state, denoted by (2). Four are the states of the *two-phase* region: the post-evaporation wave state, the upstream compression shock wave state, denoted by (3); downstream state of the shock wave, identified by (4); and the injection chamber state, denoted by (5). One observes that the state (2) is a boundary condition for the *two-phase* region. It corresponds to a quasi-parabolic surface of the liquid core. In Figure 2(a) one can observe a still photography experimentally obtained by Vieira [7], in Figure 2(b) one can observe a schematic of the phenomenon including the shock wave structure presenting the states involved in the phenomenon from the initial state until the injection chamber state, and in Figure 2(c) one can

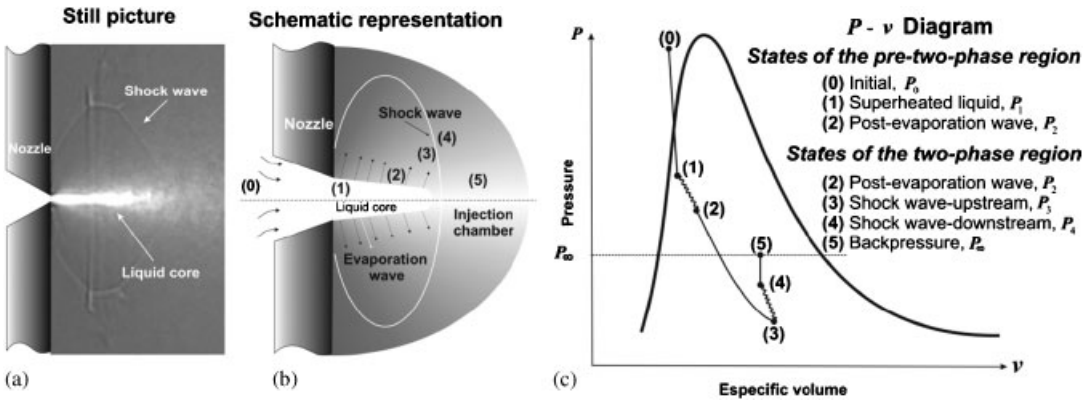

Figure 2. (a) Photograph of shock wave, Vieira [7]; (b) schematic representation of the phenomenon; and (c) thermodynamic behavior of the phenomenon in a $P-v$ diagram.

DOI: 10.1002/fld

observe the saturation curve in a $P-v$ diagram (pressure$\times$specific volume) and the thermodynamic states of the phenomenon. For a more detailed description of the *pre-two-phase* region, works by Simões-Moreira *et al.* [9], Angelo [11], and Avila *et al.* [13, 15] may be revised.

3. TWO-PHASE REGION

In our application, the flashing of metastable liquids, in a two-dimensional domain, is a steady-state problem. Vieira [6, 7] and Vieira and Simões-Moreira [8] studied it experimentally (from the reservoir to the two-phase expansion) under a steady-state regime. Furthermore, Angelo [10, 11] and Angelo and Simões-Moreira [12] carried out a numerical study of this flashing phenomenon, in the two-phase region, for the same steady-state condition, while Avila [15] studied it in the two-phase region expansion, both in steady-state or transient conditions (false transient).

3.1. Physical domain and grid

The physical domain contour is given by $\Gamma=\bigcup_{i=1}^{4}\Gamma_i$, correspondent to the two-phase region, is presented in Figure 3(a). The contour coordinates are known and denoted by (x_0, y_0).

Conformal mapping was used to obtain the numerical grid for the physical domain. One considers the following transformation $T:(\bar{x},\bar{y})\rightarrow(x,y)$, where the inverse transformation converts the physical domain into a unitary square. An elliptical boundary value problem for the coordinates $x=x(\bar{x},\bar{y})$ and $y=y(\bar{x},\bar{y})$ is represented by

$$\begin{aligned} g_{22}\frac{\partial^2 x}{\partial \bar{x}^2}-2g_{12}\frac{\partial^2 x}{\partial \bar{x}\partial \bar{y}}+g_{11}\frac{\partial^2 x}{\partial \bar{y}^2}=0 \\ g_{22}\frac{\partial^2 y}{\partial \bar{x}^2}-2g_{12}\frac{\partial^2 y}{\partial \bar{x}\partial \bar{y}}+g_{11}\frac{\partial^2 y}{\partial \bar{y}^2}=0 \end{aligned} \tag{1}$$

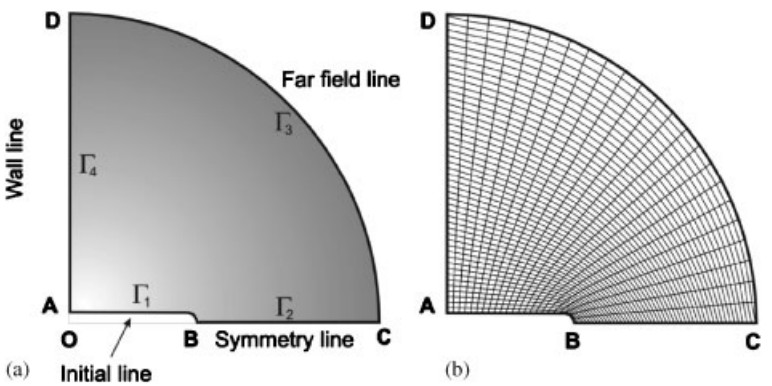

Figure 3. (a) Physical domain and (b) physical grid.

DOI: 10.1002/fld

where

$$g_{12}=\frac{\partial x}{\partial \bar{x}}\frac{\partial x}{\partial \bar{y}}+\frac{\partial y}{\partial \bar{x}}\frac{\partial y}{\partial \bar{y}},\quad g_{11}=\left(\frac{\partial x}{\partial \bar{x}}\right)^2+\left(\frac{\partial y}{\partial \bar{x}}\right)^2,\quad g_{22}=\left(\frac{\partial x}{\partial \bar{y}}\right)^2+\left(\frac{\partial y}{\partial \bar{y}}\right)^2 \tag{2}$$

with the Dirichlet boundary conditions

$$x|_\Gamma=x_0,\quad y|_\Gamma=y_0 \tag{3}$$

The solution to this problem generates a structured physical grid, as shown in Figure 3(b).

3.2. Governing equations

The flashing phenomenon of superheated liquids, for the case of inviscid fluid in a two-dimensional axisymmetric is modeled by the following conservation equations: mass conservation, momentum conservation, and energy conservation. This system formed by four equations presents five unknowns or primitive variables, as $\{\rho, u, v, p, e\}$, density, x-velocity vector, y-velocity vector, pressure and internal specific energy, respectively, where $E=\rho e+0.5\rho V^2$ is the total energy and $V=\sqrt{u^2+v^2}$ the velocity vector module. In order to solve the system of equations, we used the Lee–Kesler state equation. It is important to point out that the quality, x, is used to calculate all other thermodynamic properties.

3.2.1. Cartesian coordinates. The two-dimensional vectorial conservation laws form a system of quasi-linear partial differential equations of first order, given by

$$\frac{\partial U}{\partial t}+\frac{\partial F}{\partial x}+\frac{\partial G}{\partial y}+\frac{S}{y}=0 \tag{4}$$

where

$$U=\begin{bmatrix}\rho\\ \rho u\\ \rho v\\ E\end{bmatrix},\quad F=\begin{bmatrix}\rho u\\ \rho u^2+p\\ \rho uv\\ (E+p)u\end{bmatrix},\quad G=\begin{bmatrix}\rho v\\ \rho uv\\ \rho v^2+p\\ (E+p)v\end{bmatrix},\quad S=\begin{bmatrix}\rho v\\ \rho uv\\ \rho v^2\\ (E+p)v\end{bmatrix} \tag{5}$$

One designates U, the unknown variable of state (conserved variables), F and G the vectorial flux functions, or simply the flux vectors, and S represents a source term.

3.2.2. Orthogonal curvilinear coordinates. The conservational laws of Fluid Dynamics are valid for any coordinates system. The conservation equations are then transformed from Cartesian coordinates (x, y) into Orthogonal Curvilinear coordinates (ξ, η). As a result one has the computational domain that is a two-dimensional unitary square in (ξ, η) coordinates, with the boundary given by $\Gamma'=\bigcup_{i=1}^{4}\Gamma'_i$, as seen in Figure 4(a).

DOI: 10.1002/fld

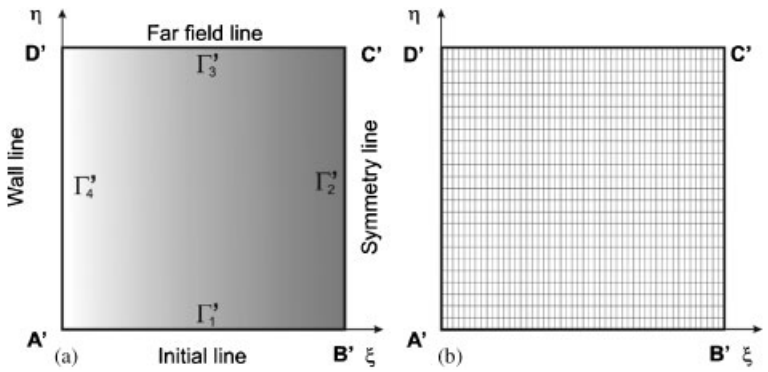

Figure 4. (a) Computational domain and (b) computational grid.

The metrics of the orthogonal curvilinear system are

$$\xi_x = Jy_\eta, \quad \xi_y = -Jx_\eta, \quad \eta_x = -Jy_\xi, \quad \eta_y = Jx_\xi \tag{6}$$

where J is the Jacobian and $\{x_\xi, y_\xi, x_\eta, y_\eta\}$ are approximated, for instance by means of central difference scheme. Finally the system of conservational laws, in the computational domain, is given by

$$\frac{\partial \hat{U}}{\partial t} + \frac{\partial \hat{F}}{\partial \xi} + \frac{\partial \hat{G}}{\partial \eta} + \hat{S} = 0, \qquad \hat{U} = \frac{U}{J}, \quad \hat{G} = \frac{1}{J}(\eta_x F + \eta_y G), \quad \hat{F} = \frac{1}{J}(\xi_x F + \xi_y G), \quad \hat{S} = \frac{S}{Jy} \tag{7}$$

where $\hat{U}$ is the conserved variables vector, $\hat{F}$ and $\hat{G}$ the flux vectors and $\hat{S}$ the source term, all in the computational domain.

3.3. Boundary conditions

In the physical domain, the known boundary conditions are: *initial line* (velocity, Mach number, M, pressure, temperature, density, and quality), in the *symmetry line* (impervious condition), in the *far-field line* (far-field pressure, p_∞), and *wall line* (impervious condition). Following are the boundary conditions:

$$\Gamma_1 : u = \left[\frac{W_2}{\sin(\theta+\beta)}\right]\cos(\theta), \quad v = \left[\frac{W_2}{\sin(\theta+\beta)}\right]\sin(\theta), \quad M = 1, \quad p = p_2, \quad T = T_2$$

$$\rho = \frac{1}{v_2}, \quad x = x_2, \quad \Gamma_2 : u \neq 0, \quad v = 0, \quad \Gamma_3 : p = p_\infty, \quad \Gamma_4 : u = 0, \quad v \neq 0$$

where W_2 is the normal velocity component after the evaporation wave, β is the wave angle, θ is the rotation angle, and v_2 is its specific volume. The subscript '2' indicates the thermodynamic

DOI: 10.1002/fld

values for the state post-wave of evaporation, as shown in Avila *et al.* [13]. At the boundary contours $\{\Gamma_2, \Gamma_3, \Gamma_4\}$, in order to obtain the thermodynamic properties, the *numerical boundary conditions* are evaluated with order zero and one.

4. NUMERICAL SOLUTION: NON-STATIONARY METHOD

4.1. Flux vector splitting

The hyperbolic conservational two-dimensional system of equations for inviscid fluid flows in gas dynamics have used the *splitting method* for the flux vectors, which apply the homogeneity principle and the theory of the eigenvalues, for the F and G flux vectors, see Steger and Warming [17]. Let one consider the system of conservation laws equations, Equation (4). Then the flux vectors, based on the homogeneity condition, may be expressed as

$$\begin{aligned} F &= AU \\ G &= BU \end{aligned} \tag{8}$$

where the Jacobian matrices A and B are given by

$$A = \frac{\partial F}{\partial U}, \quad B = \frac{\partial G}{\partial U} \tag{9}$$

Substituting Equation (8) into Equation (7), the flux vectors, $\hat{F}$ and $\hat{G}$, are given by

$$\hat{F} = (\xi_x A + \xi_y B)\hat{U}, \quad \hat{G} = (\eta_x A + \eta_y B)\hat{U} \tag{10}$$

One will split the flux vectors $\hat{F}$ and $\hat{G}$, but first the Jacobian of the matrices $\hat{A}$ and $\hat{B}$ are defined by

$$\hat{A} = \xi_x A + \xi_y B, \quad \hat{B} = \eta_x A + \eta_y B \tag{11}$$

The evaluation of the Jacobian matrices of the flashing process of metastable liquid jets is revised by Avila [15].

4.2. Dispersion-controlled dissipative (DCD) scheme

The dispersion-controlled dissipative (DCD) scheme is second order and belongs to the class of the non-oscillatory shock capturing process. This class is different from conventional schemes with dissipation, as the dissipative terms of the modified equations are not considered during the scheme construction of the schemes, in order to avoid non-physical oscillations that might occur during shock waves simulation. This method is a mixture of the *Lax-Wendroff* and *Beam-Warming* with a 'min mod' flux function.

Jiang [18] has conducted systematic tests of the dispersion-controlled principle since his first work (1993), and he has published the conditions of dispersion for the non-oscillatory shock capturing scheme. This principle aims at the removal of non-physical oscillations using dispersion characteristics instead of adding artificial viscosity in order to eliminate oscillations as is done by the conventional schemes.

DOI: 10.1002/fld

The DCD scheme was originally elaborated for the finite differences method; however, it has been extended to other methods such as finite volumes or finite elements. High-order scheme have been implemented.

As examples, many applications were conducted in problems with toroidal shocks in cylindrical chambers [19], gas combustion shock waves [20].

The DCD scheme has been implemented and the computational code has been called *DCD-2D v1*.

4.2.1. Finite differences formulation. In the computational domain, the finite differences equations for Equation (7) spatially discredited using the DCD scheme [16] are given in their semi-discrete form by

$$\left[\frac{\partial \hat{U}}{\partial t}\right]^n_{i,j} = -\frac{1}{\Delta\xi}(\hat{H}^n_{i+1/2,j} - \hat{H}^n_{i-1/2,j}) - \frac{1}{\Delta\eta}(\hat{P}^n_{i,j+1/2} - \hat{P}^n_{i,j-1/2}) - \hat{S}^n_{i,j} \tag{12}$$

where $\Delta\xi$ is the length in the direction ξ and $\Delta\eta$ the length in the direction η of an element of the computational grid as shown in Figure 4(b), and

$$\begin{aligned} \hat{H}^n_{i+1/2,j} &= \hat{F}^+_{i+(1/2)L,j} + \hat{F}^-_{i+(1/2)R,j}, \quad \hat{P}^n_{i,j+1/2} = \hat{G}^+_{i,j+(1/2)L} + \hat{G}^-_{i,j+(1/2)R} \\ \hat{H}^n_{i-1/2,j} &= \hat{F}^+_{i-(1/2)L,j} + \hat{F}^-_{i-(1/2)R,j}, \quad \hat{P}^n_{i,j-1/2} = \hat{G}^+_{i,j-(1/2)L} + \hat{G}^-_{i,j-(1/2)R} \end{aligned} \tag{13}$$

where $\hat{F}^\pm$ and $\hat{G}^\pm$ are the numerical fluxes vectors with respect to fluxes vectors F and G, respectively. Thus, for example, $\hat{F}^\pm$ is defined as

$$F^+_{i+(1/2)L,j} = F^+_{i,j} + \tfrac{1}{2}\Phi^+_A[\text{minmod}(\Delta F^+_{i-1/2,j}, \Delta F^+_{i+1/2,j})]$$

$$F^-_{i+(1/2)R,j} = F^-_{i+1,j} - \tfrac{1}{2}\Phi^-_A[\text{minmod}(\Delta F^-_{i+1/2,j}, \Delta F^-_{i+3/2,j})]$$

$$F^+_{i-(1/2)L,j} = F^+_{i-1,j} + \tfrac{1}{2}\Phi^+_A[\text{minmod}(\Delta F^+_{i-3/2,j}, \Delta F^+_{i-1/2,j})]$$

$$F^-_{i-(1/2)R,j} = F^-_{i,j} - \tfrac{1}{2}\Phi^-_A[\text{minmod}(\Delta F^-_{i-1/2,j}, \Delta F^-_{i+1/2,j})]$$

where the variations numerical fluxes vectors are given by

$$\Delta F^+_{i-3/2,j} = F^+_{i-1,j} - F^+_{i-2,j}, \quad \Delta F^-_{i-1/2,j} = F^-_{i,j} - F^-_{i-1,j}$$

$$\Delta F^+_{i-1/2,j} = F^+_{i,j} - F^+_{i-1,j}, \quad \Delta F^-_{i+1/2,j} = F^-_{i+1,j} - F^-_{i,j}$$

$$\Delta F^+_{i+1/2,j} = F^+_{i+1,j} - F^+_{i,j}, \quad \Delta F^-_{i+3/2,j} = F^-_{i+2,j} - F^-_{i+1,j}$$

The evaluations for $\hat{G}^\pm$ are analogous. In Figure 5, one shows the computational cell to determine the variations of the numerical flux vector.

The matrices, Φ, related to the Jacobian matrices A and B are given by

$$\Phi^\pm_A = I \mp \beta\Lambda^\pm_A, \quad \Phi^\pm_B = I \mp \beta\Lambda^\pm_B \tag{14}$$

DOI: 10.1002/fld

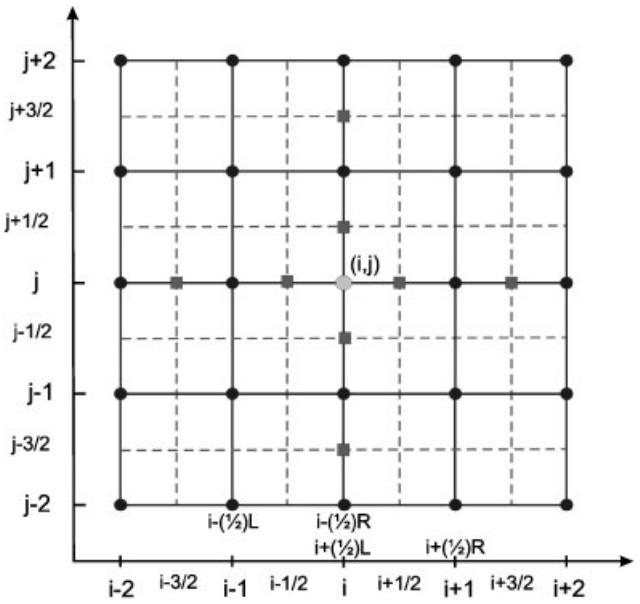

Figure 5. Computational cell.

where $\Lambda_A^{\pm}$ and $\Lambda_B^{\pm}$ are the diagonal matrices formed by the eigenvalues of A and B, respectively. I is the identity matrix and β a parameter defined by

$$\beta = \frac{\Delta t}{\Delta \xi} \tag{15}$$

where Δt is the time step size. The limiting function 'minmod' is defined by

$$\text{minmod}(x, y) = \begin{cases} \text{sgn}(x)\min\{|x|, |y|\} & \text{if } \text{sgn}(x) = \text{sgn}(y) \\ 0 & \text{if } \text{sgn}(x) \neq \text{sgn}(y) \end{cases} \tag{16}$$

where 'sgn' is the sign function.

4.2.2. Temporal discretization. The time step size Δt, according to Peyret and Taylor [21], in the computational domain, is given by

$$\Delta t = \frac{C_0}{\dfrac{\|u\|}{\Delta \xi} + \dfrac{\|v\|}{\Delta \eta} + \|c\| \sqrt{\dfrac{1}{\Delta \xi^2} + \dfrac{1}{\Delta \eta^2}}} \tag{17}$$

where C_0 is a positive constant ($C_0 = 5, 6$ in this work). c is the sound speed in the two-phase flow. $\|\cdot\|$ is the Euclidian norm of a matrix, for instance, the velocity vector component $u = (u_{ij})_{N \times M}$, which is evaluated in all nodes of the computational domain. In the temporal discretization the second-order Runge–Kutta method was used.

DOI: 10.1002/fld

5. NUMERICAL RESULTS: FALSE-TRANSIENT METHOD

In this work, as means of validating the *DCD-2D v1* computer code, according the false-transient method, one analyzes the convergent–divergent nozzle. For other works revise Avila [15]. Notwithstanding, the problem to be solved and principal objective of this investigation is the steady-state flashing of metastable liquid jets in the two-phase region or the two-phase expansion problem.

Used grids are some geometrical and others generated by means of bi univocal transformations of the coordinates. The subscript used to identify the grid dimensions with $(N+2)\times(M+2)$ nodes is $(i=\overline{0,N+1};\ j=\overline{0,M+1})$, where i denote the points along a parallel line to the initial line, j lines that follow approximately the streamlines of this flow, and M, N integer positive numbers. Initial conditions may be arbitrary, but cannot be unrealistic. The *DCD-2D v1* code supports all these initial conditions; however, to speed up the process of capturing one includes shock waves close to the beginning of the flow. Numerical convergence and efficient calculations are supported with these cares.

The expression '*EE_GP*' means that one has used perfect gas state equation or '*EE_GP**' when the equation is in the form of $p=(\gamma-1)\rho e$, where γ is the specific heat ratio equal to 1.40 for the calculation of one thermodynamic variable.

The system of units in this work is from the International System, SI, and each test was running with a AMD Atlon (tm) 64X2 Dual Core Processor 5200^{+} 2.73 GHz computer.

5.1. Convergent–divergent nozzle

The convergent–divergent nozzle problem (or De Laval) in steady-state regime is quasi one-dimensional. The region of this nozzle is given by

$$D=\{(x,y)\in R^2 : 0\leqslant x\leqslant 3 \wedge |y|\leqslant (1/8)[1+2.2(x-1.5)^2]\} \tag{18}$$

where the area ratio is $A_s/A^*=5.95$, with A^* the throat area and A_s the exit area. This problem is identical to the example presented by Anderson [22, p. 356]. In Figure 6 one has the grid for the De Laval domain, D.

The physical and numerical boundary conditions are given in Table I. The entrance line, the exit line, the curved lines for the upper and lower walls are the segments: $\overline{\mathrm{AB}}$, $\overline{\mathrm{CD}}$, $\widehat{\mathrm{BC}}$, and $\widehat{\mathrm{DA}}$, respectively. The reservoir conditions are: $p_0=600\mathrm{E}{+}03$ and $T_0=320$ and $c=\sqrt{\gamma(p/\rho)}$.

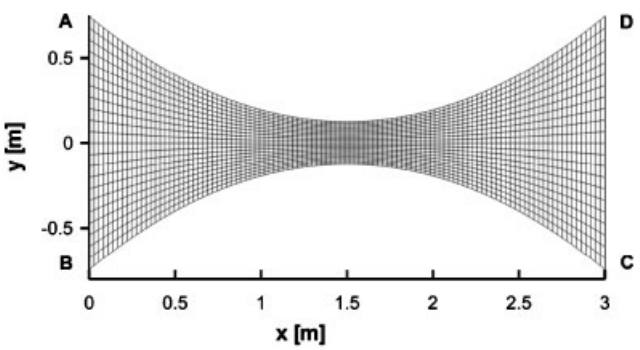

Figure 6. Convergent–divergent nozzle grid.

DOI: 10.1002/fld

In Table II the analytical and numerical solutions are presented for the exit station of De Laval. As well, it is shown the err, the shock wave location (s.w.l, in (m)), and the CPU time (h:min:s). Observe that just the pressure has a relatively high err.

The Figures 7(a) and (b) represent the pressure and Mach number contours, respectively. In each one observes the formation of a shock wave in the point 2.15 m.

The Figures 8(a) and (b) represent, respectively, pressure and Mach number distributions.

Table I. Physical and numerical boundary conditions for the convergent–divergent nozzle.

	$\overline{AB}$	$\widehat{BC}$	$\widehat{DA}$	$\overline{CD}$
M	0.0982	V/c	V/c	V/c
T	T_0	$T_{N+1,j}=T_{N,j}$	$T_{0,j}=T_{1,j}$	EE_GP
p	p_0	$p_{N+1,j}=p_{N,j}$	$p_{0,j}=p_{1,j}$	$0.678\times p_0$
ρ	EE_GP	EE_GP	EE_GP	$\rho_{i,M+1}=\rho_{i,M}$
e	EE_GP*	EE_GP*	EE_GP*	EE_GP*
u	$M\times c$	$u_{N+1,j}=u_{N,j}$	$u_{0,j}=u_{1,j}$	$u_{i,M+1}=u_{i,M}$
v	0	$v_{N+1,j}=v_{N,j}$	$v_{0,j}=v_{1,j}$	$v_{i,M+1}=v_{i,M}$

Table II. Analytical and numerical solution for the convergent–divergent nozzle.

	Analytical solution	Numerical solution		
	Exit		Exit	Err %
M	0.143		0.140	2.1
T/T_0	0.996		0.985	1.1
p/p_0	0.678		0.791	16.7
s.w.l		2.15		
CPU		00:44:43		

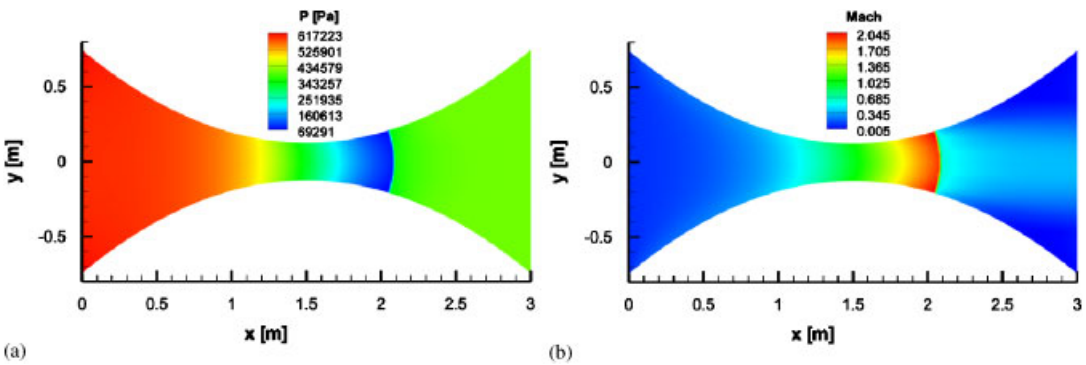

Figure 7. (a) Pressure contours and (b) Mach number contours.

DOI: 10.1002/fld

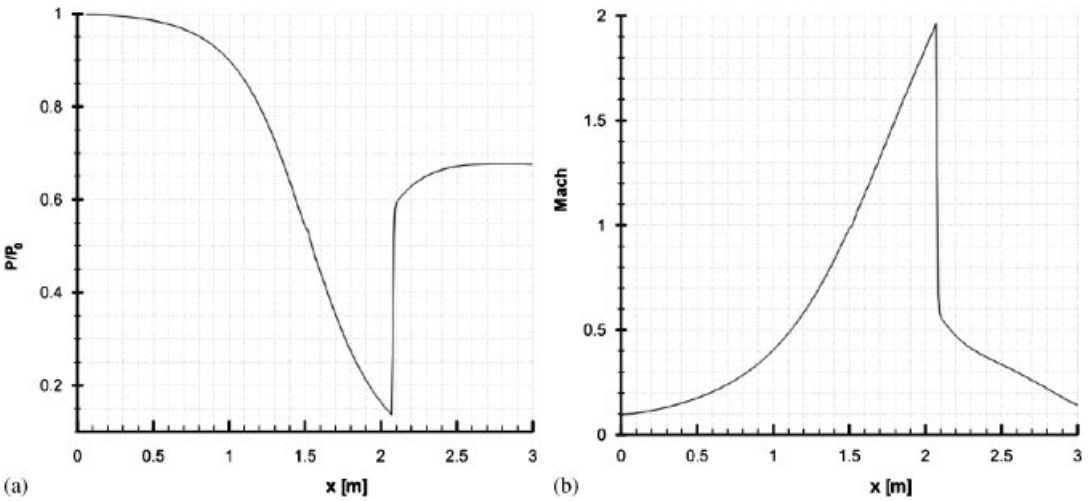

Figure 8. (a) Pressure profile and (b) Mach number profile.

Table III. Grid size, radius $R_f = 22E-03$ m.

Grid type	Initial line M	Wall line N	Nodes total $M \times N$
A	77	161	12 397

Table IV. Boundary conditions and numerical solution.

Reservoir conditions	Boundary conditions		
$P_0 = 503, 4E+03, T_0 = 368.55$	*Initial line*	*Far-field line*	Numerical solution
M	1		
T	331.4		
p	26 862	8000	
x	0.2965		
V	73.7		
sw.l			$r_1 = 16.2E-03$ $r_2 = 14.7E-03$
CPU			04:48:23

5.2. *Two-phase expansion*

The two-phase expansion problem is a steady-state phenomenon in a 2D axisymmetric domain, in particular the two phase region. The test fluid was the isooctane (C_8H_{18}) and the used state equation was obtained from the Lee–Kesler equation. The technique used to solve the mathematical problem derived from it was the false-transient method. Several tests were conducted, but in this work it is only presented the *Test 11*, for other results one is asked to see Avila [14]. The two-phase

DOI: 10.1002/fld

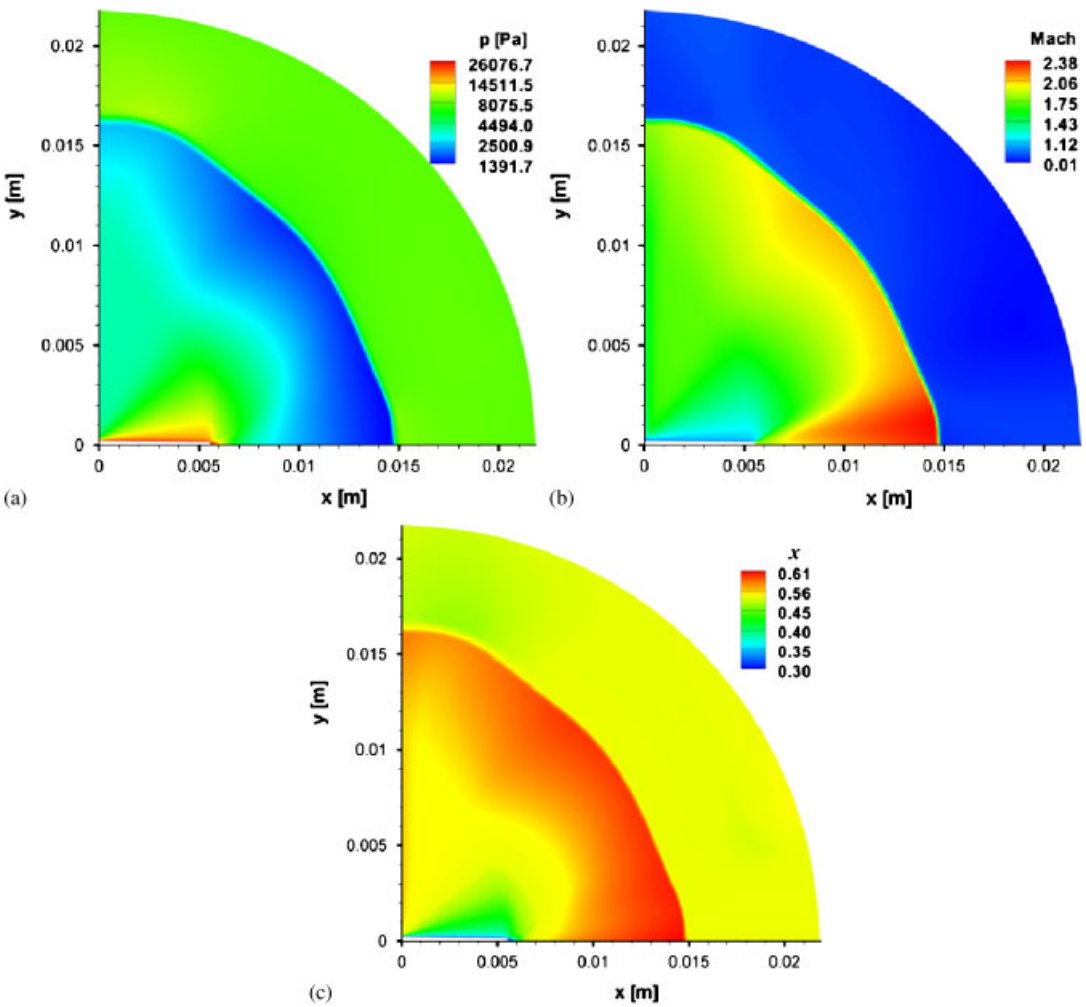

Figure 9. (a) Pressure contours; (b) Mach number contours; and (c) quality contours.

region has a radius $R_f = 22\text{E}-03\,\text{m}$ (see Figure 3(a), $R_f = \overline{\text{OC}} = \overline{\text{OD}}$). The shock wave length (sw.l) is given by: the radial length, r_1 (orthogonal projection of far most point of the wave in the x axis), and axial length, r_2 (origin to interception of wave with x axis). The superficial area of the liquid core has a more or less parabolic shape (Figure 2(b)); one calls it the initial area and we will denote it by A_0, and the superficial area of the hemi-sphere (two-phase region) is called by far-field area and denoted by A_∞. In this test, the initial and far-field areas are, respectively, $A_0 = 1.63\text{E}-05\,\text{m}^2$, $A_\infty = 2.98\text{E}-03\,\text{m}^2$. The used grid has $(M \times N)$ nodes, see Table III.

The reservoir conditions, boundary conditions, and numerical results can be seen in Table IV.

Figures 9(a)–(c) present pressure contours, Mach numbers, and quality, respectively. Observe that at the extremes of *initial line* expansion is fast, while in its sides the same expansion is slower, forming a cone with vertex at the nozzle entrance.

DOI: 10.1002/fld

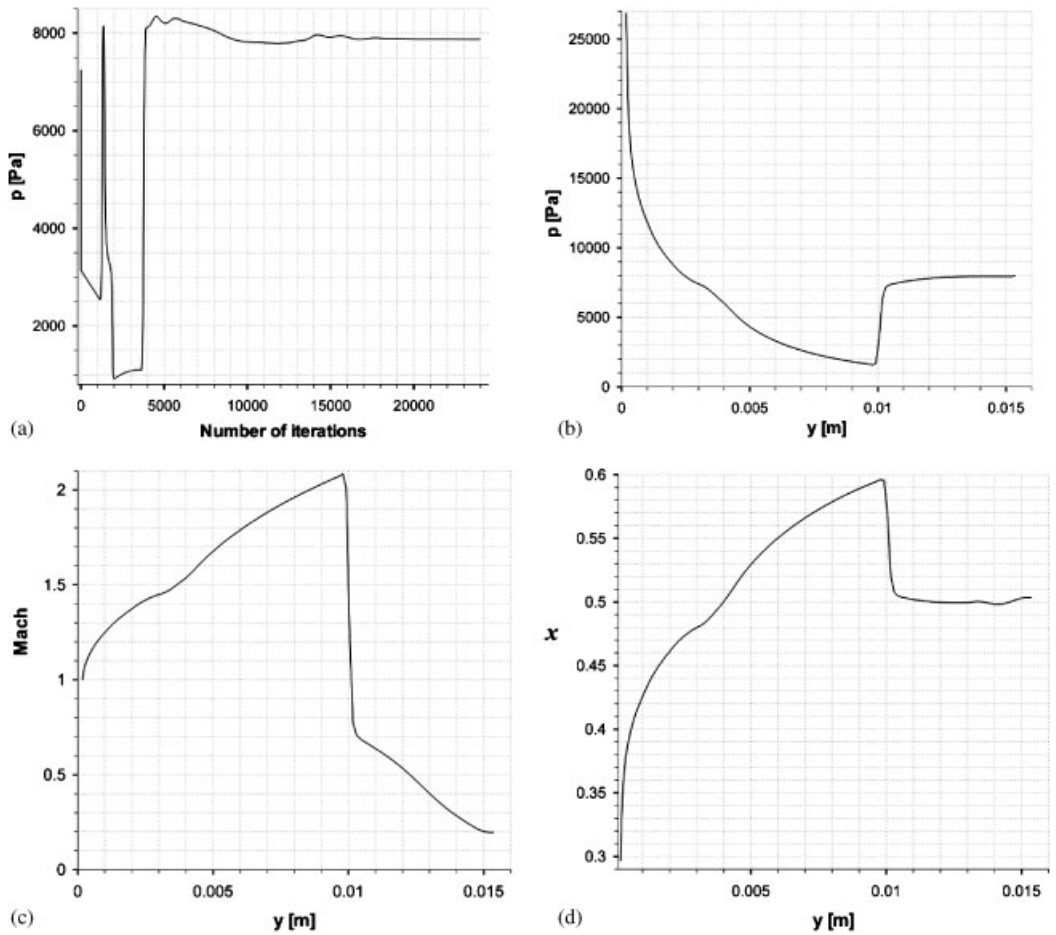

Figure 10. (a) Pressure versus number of iterations for a fixed grid node; (b) pressure profile; (c) Mach number profile; and (d) quality profile.

In Figure 10(a) one has the behavior during calculations of the point (50.184) of the grid. One may see that in the steady state the fluid reached at this point after 24 000 iterations, after a computational time of 04 h 48 min 23 s. The pressure at this point reaches the value of 7868.2 Pa. The following Figures 10(b)–(d) show pressure, Mach number, and quality profiles, respectively. These profiles correspond to the grid line ($i_0 = 39$; $j = \overline{0.160}$). Finally, in Figure 11 one has the surface of pressure contours in 3D.

The CDC scheme was implemented and applied to numerically solve the flashing of superheated jets in the two-phase part of this flow. The results were very encouraging as, with some simplification hypothesis, gave results that compared very well with the experimental measurements and photos. The advantage of this method is that it gives transient solutions, as indicated in the references cited in Section 4.2. This fact has encouraged us to pursue the solution for the whole domain, even without all experimental results.

DOI: 10.1002/fld

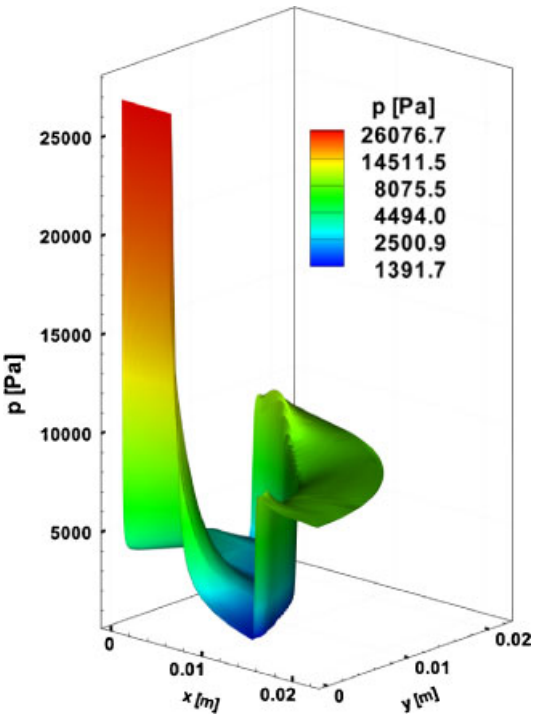

Figure 11. Pressure contours in 3D.

6. CONCLUSIONS

For the false-transient method applied to flashing of metastable liquids in the two-phase region, the *DCD-2D v1* code directly captures the shock wave without a post-processing scheme as did the codes (*ShoWPhasT-2D v1* and *ShoWPhasT-2D v2*). However, it does not give yet good results for the shock wave length when compared with these last ones. This method allows the determination of velocity profiles and thermodynamic field across all the two-phase region of the flow. The quality distribution was also determined.

REFERENCES

1. Ogle RA, Megerle MV, Morrison DR, Carpenter AR. Explosion caused by flashing liquid in a process vessel. *Journal of Hazardous Materials* 2004; **115**:133–140.
2. Macphee AG *et al.* X-ray imaging of shock waves generated by high-pressure fuel sprays. *Science* 2002; **295**(1261).
3. Rochette D, Clain S, Bussière W, Gentils F. Two-dimensional modelling of internal arc effects in an enclosed MV cell provided with a protection porous filter. *Journal of Physics D*: *Applied Physics* 2007; **40**:3137–3144.
4. Simões-Moreira JR. Adiabatic evaporation waves. *Ph.D. Thesis*, Rensselaer Polytechnic Institute, Troy, NY, 1994.
5. Kurschat T, Chaves H, Meier GEA. Complete adiabatic evaporation of highly superheated liquid jets. *Journal of Fluid Mechanics* 1992; **236**:43–59.
6. Vieira MM. Estudo experimental de jatos evaporativos. *Dissertation* (*Master*), Mechanical Engineering Department, Escola Politécnica, Universidade de São Paulo, São Paulo, 1999; 228 (in Portuguese).

DOI: 10.1002/fld

7. Vieira MM. Estudo Experimental da Evaporação de Jatos de Iso-octano Superaquecido. *Ph.D. Thesis*, Mechanical Engineering Department, Escola Politécnica, Universidade de São Paulo, São Paulo, 2005; 372 (in Portuguese).
8. Vieira MM, Simões-Moreira JR. Low pressure flashing mechanisms in iso-octane liquid jets. *Journal of Fluid Mechanics* 2007; **572**:121–144.
9. Simões-Moreira JR, Vieira MM, Angelo E. Highly expanded flashing liquid jets. *Journal of Thermophysics and Heat Transfer* 2002; **16**(3):415–424.
10. Angelo E. Estudo numérico de jatos evaporativos. *Dissertation* (*Master*), Mechanical Engineering Department, Escola Politécnica, Universidade de São Paulo, São Paulo, 2000; 148 (in Portuguese).
11. Angelo E. Análise numérica da dinâmica da expansão de líquidos superaquecidos em evaporação rápida. *Ph.D. Thesis*, Mechanical Engineering Department, Escola Politécnica, Universidade de São Paulo, São Paulo, 2004; 199 (in Portuguese).
12. Angelo E, Simões-Moreira JR. Numerical solution of highly expanded flashing liquid jets. *Journal of Thermophysics and Heat Transfer* 2007; **21**(2):379–391.
13. Avila JAJ, Vieira MM, Pimenta MM, Simões-Moreira JR. Liquid jet flashing into a low pressure environment: a numerical solution. *39th AIAA Thermophysics Conference*, Miami, FL, June 2007; *AIAA 2007-4162*.
14. Avila JAJ, Pimenta MM, Simões-Moreira JR. Evaporação rápida em jatos de líquidos metaestáveis: uma abordagem numérica. *CONEM 2008*: *V Congresso Nacional de Engenharia Mecânica*, Salvador–Bahia–Brasil, 25–28 August 2008 (in Portuguese).
15. Avila JAJ. Solução Numérica em jatos de líquidos metaestáveis com evaporação rápida. *Ph.D. Thesis*, Escola Politécnica, Universidade de São Paulo, São Paulo, 2008; 144 (in Portuguese).
16. Jiang Z. Study on the finite difference theory and numerical methods of weak solution problems. *Ph.D. Thesis*, Peking University, Beijing, China, 1993.
17. Steger JF, Warming RF. Flux vector splitting of the inviscid gasdynamic equations with applications to finite difference methods. *Journal of Computational Physics* 1981; **40**:263–293.
18. Jiang Z. On dispersion-controlled principles for non-oscillatory shock-capturing schemes. *Acta Mechanica Sinica* 2004; **20**(1):1–15.
19. Teng H, Jiang Z, Han Z, Hosseini SHR, Takayama K. Numerical investigation of toroidal shock wave focusing in a cylindrical chamber. *Shock Wave* 2005; **14**(4):299–305.
20. Teng H, Wang C, Deng B, Jiang Z. Ignition characteristics of the shock wave focusing in combustive gases. *Chinese Journal of Theoretical and Applied Mechanics* 2007; **39**(2):171–180.
21. Peyret R, Taylor TD. *Computational Methods for Fluid Flow*. Springer: New York, 1983; 358.
22. Anderson JD. *Computational Fluid Dynamics*: *The Basics with Applications*. McGraw-Hill: New York, 1995; 547.

DOI: 10.1002/fld